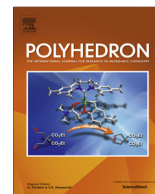




Contents lists available at ScienceDirect

Polyhedron

journal homepage: [www.elsevier.com/locate/poly](http://www.elsevier.com/locate/poly)

# Synthesis and redox properties of mono-, di- and tri-metallic platinum-ethynyl complexes based on the *trans*-Pt(C<sub>6</sub>H<sub>4</sub>N{C<sub>6</sub>H<sub>4</sub>OCH<sub>3</sub>-4})<sub>2</sub>(C≡CR)(PPh<sub>3</sub>)<sub>2</sub> motif

 Kevin B. Vincent<sup>a</sup>, Matthias Parthey<sup>b</sup>, Dmitry S. Yufit<sup>a</sup>, Martin Kaupp<sup>b,\*</sup>, Paul J. Low<sup>a,c,\*</sup>
<sup>a</sup> Department of Chemistry, Durham University, South Rd, Durham DH1 3LE, UK

<sup>b</sup> Technische Universität Berlin, Institut für Chemie, Theoretische Chemie/Quantenchemie, Sekr. C7, Strasse des 17. Juni 135, 10623 Berlin, Germany

<sup>c</sup> School of Chemistry and Biochemistry, University of Western Australia, 35 Stirling Highway, Crawley, WA 6009, Australia

## ARTICLE INFO

## Article history:

Received 10 March 2014

Accepted 14 April 2014

Available online xxxxx

Dedicated to Professor Claude Lapinte, in recognition of his outstanding career, and with thanks for his generosity and kindness over many years of fruitful and enjoyable collaboration

## Keywords:

Mixed-valence

Spectroelectrochemistry

DFT

Triarylamine

Platinum

## ABSTRACT

The Pt-halide complex *trans*-Pt{C<sub>6</sub>H<sub>4</sub>NAr<sub>2</sub>}(PPh<sub>3</sub>)<sub>2</sub> (Ar = C<sub>6</sub>H<sub>4</sub>OMe-4, **3**) was prepared by oxidative addition of N(C<sub>6</sub>H<sub>4</sub>I)Ar<sub>2</sub> (**2**) to Pt(PPh<sub>3</sub>)<sub>4</sub>. Reactions of *trans*-Pt{C<sub>6</sub>H<sub>4</sub>NAr<sub>2</sub>}(PPh<sub>3</sub>)<sub>2</sub> (**3**) with 1-alkynes under CuI catalysed dehydrohalogenation conditions allows the preparation of a range of platinum ethynyl compounds containing up to four redox-active triarylamine centres. The compounds *trans*-Pt(C≡CAr)(C<sub>6</sub>H<sub>4</sub>NAr<sub>2</sub>)(PPh<sub>3</sub>)<sub>2</sub> (**4a**), *trans*-Pt(C≡CC<sub>6</sub>H<sub>4</sub>NAr<sub>2</sub>)(C<sub>6</sub>H<sub>4</sub>NAr<sub>2</sub>)(PPh<sub>3</sub>)<sub>2</sub> (**4b**), {*trans*-Pt(C<sub>6</sub>H<sub>4</sub>NAr<sub>2</sub>)(PPh<sub>3</sub>)<sub>2</sub>}<sub>2</sub> (μ-C≡C-1,4-C<sub>6</sub>H<sub>4</sub>C≡C) (**5**) and N{C<sub>6</sub>H<sub>4</sub>C≡CPt(C<sub>6</sub>H<sub>4</sub>NAr<sub>2</sub>)(PPh<sub>3</sub>)<sub>2</sub>}<sub>3</sub> (**6**) undergo a single electrochemical event for each chemically distinct type of triarylamine in the molecular backbone. The complete reversibility of the larger systems means that they can be used for charge storage materials capable of releasing up to four electrons. A combination of electrochemical, spectroelectrochemical and quantum chemical analyses reveal weak electronic coupling between the amine moieties in the redox products derived from one-electron oxidation.

© 2014 Elsevier Ltd. All rights reserved.

## 1. Introduction

Complexes of general form PtX(Ar')(PR<sub>3</sub>)<sub>2</sub> (X = halide, pseudo halide; Ar' = aryl; R = aromatic, alkyl) have a long history, and can be prepared by numerous synthetic methods, including reactions of [PtX<sub>2</sub>{bis(olefin)}] with aryl Grignard reactions and phosphine [1–3], or Pt(X)<sub>2</sub>(PR<sub>3</sub>)<sub>2</sub> with ArLi [4], by disproportionation reactions of PtCl(MPh<sub>2</sub>)(PPh<sub>3</sub>)<sub>2</sub> (M = Sn, Pb) [5], reaction of *cis*-PtPh(PPh<sub>3</sub>)<sub>2</sub> (PbPh<sub>3</sub>) with Br<sub>2</sub> or HBr [6], decarbonylation of PtX(COAr)(PR<sub>3</sub>)<sub>2</sub> [7], ligand exchange reactions of {Pt(μ-Cl)(tht)(C<sub>6</sub>F<sub>5</sub>)<sub>2</sub>} [8], and perhaps most simply by oxidative addition of arylhalides to Pt(PR<sub>3</sub>)<sub>n</sub> (R = Ph, Et; n = 3, 4) [9–13]. These aryl platinum(II) complexes have served as models through which to explore key reaction steps in various catalytic transformations [14–17], and as structurally well defined building blocks for the assembly of molecular nanostructures [18–20], scaffolds and redox-innocent end-caps for polyynes,

some of quite extraordinary length [3,8,21–26]. Alkynyl complexes *trans*-Pt(C≡CR)(Ar')(PR<sub>3</sub>)<sub>2</sub> have also demonstrated a range of interesting and potentially useful optoelectronic properties, leading to the design of soluble and processable materials with low band-gaps for solar cell applications [27–34], and significant two-photon absorption cross-sections [35], whilst the heavy atom effect leads to effective intersystem crossing [36] and efficient triplet sensitised processes such as visible light induced ring-closing of Iri-style molecular switches [37], efficient optical limiting [38] and (electro)phosphorescence [39–42]. The preparation of a penta-(platinum alkynyl) complex of corannulene further demonstrates the vast scope for use of the *trans*-PtXAr'(PR<sub>3</sub>)<sub>2</sub> motif to assemble and stabilise complex structures [43].

We were attracted to the synthetic, structural and electronic properties of Pt(II) aryl complexes as potential scaffolds for the construction of structures in which two or more organic electrophores, specifically triarylamine moieties, could be linked into larger structures of well defined geometry with a view to exploring further examples of metal-bridged organic mixed-valence compounds [44,45,46]. We report here the synthesis of the redox-active building block *trans*-Pt{C<sub>6</sub>H<sub>4</sub>NAr<sub>2</sub>}(PPh<sub>3</sub>)<sub>2</sub> (**3**, Ar = C<sub>6</sub>H<sub>4</sub>OMe-4), and its use in the preparation of mono-, bi- and trimetallic complexes from

\* Corresponding authors. Address: School of Chemistry and Biochemistry, University of Western Australia, 35 Stirling Highway, Crawley, WA 6009, Australia. Tel.: +61 (0)8 6488 3045; fax: +61 (0)8 6488 7330 (P.J. Low).

E-mail addresses: [martin.kaupp@tu-berlin.de](mailto:martin.kaupp@tu-berlin.de) (M. Kaupp), [paul.low@uwa.edu.au](mailto:paul.low@uwa.edu.au) (P.J. Low).

CuI catalysed reactions with terminal alkynes. Electrochemical and spectroelectrochemical investigations, supported by DFT calculations on representative examples, have been used to explore the redox chemistry and electronic structures of these complexes and their redox products. These studies reveal sequential oxidation of the  $\{\text{Ar}_2\text{NC}_6\text{H}_4-\}$  and  $\{-\text{C}\equiv\text{C}-\text{C}_6\text{H}_4\text{NAr}_2\}$  centres, which are only weakly coupled through the *trans*-Pt(PPh<sub>3</sub>)<sub>2</sub> bridge.

## 2. Results and discussion

### 2.1. Syntheses

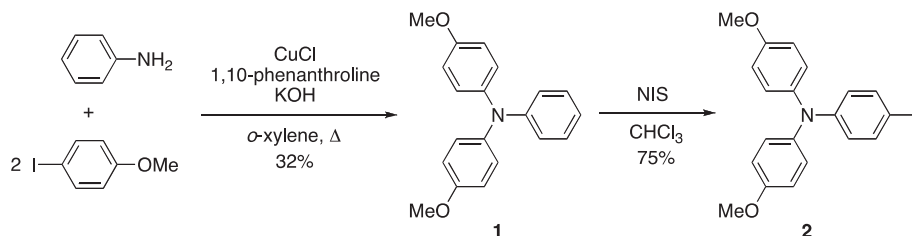
The key triarylamine building blocks **1** [47] and **2** [48,49] were assembled using the sequence of Ullmann and iodination reactions as illustrated in Scheme 1. These compounds were characterised in the usual manner by <sup>1</sup>H and <sup>13</sup>C NMR spectroscopy and EI-mass spectrometry, with the data fully consistent with that previously reported.

Compound **2** reacted smoothly with Pt(PPh<sub>3</sub>)<sub>4</sub> [50] in refluxing toluene to give *trans*-PtI(C<sub>6</sub>H<sub>4</sub>NAr<sub>2</sub>)(PPh<sub>3</sub>)<sub>2</sub> (**3**) in excellent (95%) isolated yield (Scheme 2). The *trans* geometry of **3** was established by the observation of a singlet in the <sup>31</sup>P NMR spectrum at  $\delta$  20.67 ppm, with Pt satellites ( $J_{\text{Pt-P}} = 3074$  Hz). The complex was further characterised by <sup>1</sup>H and <sup>13</sup>C NMR spectroscopy, which were fully assigned on the basis of NOESY, COSY, HSQC and HMBC methods. MALDI-MS and elemental analytical results were also fully consistent with the proposed structure.

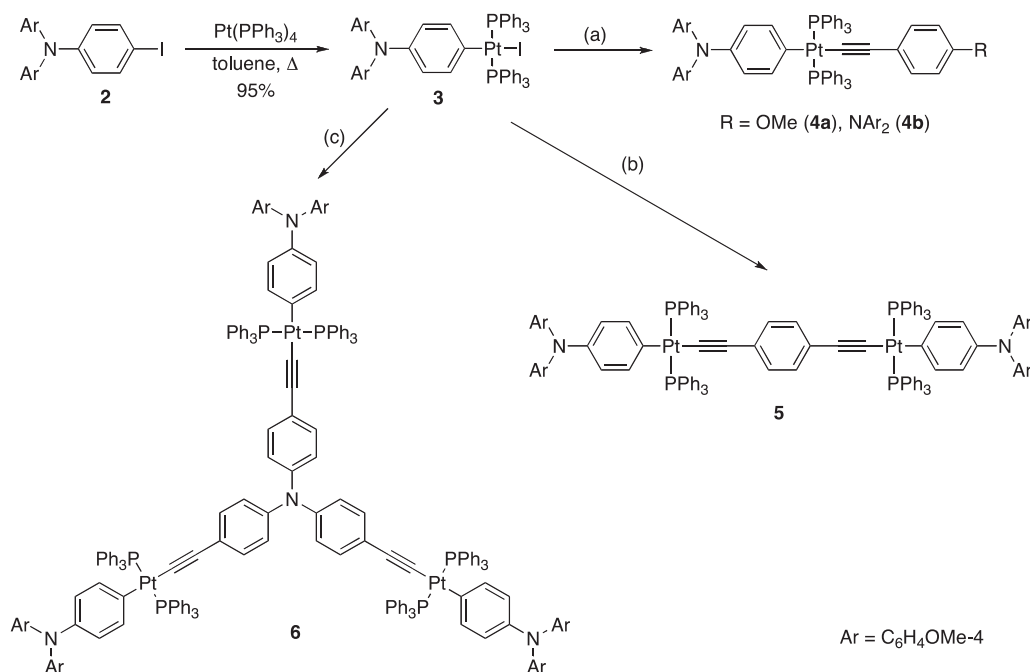
Complexes of general form *trans*-PtX(Ar')(PR<sub>3</sub>)<sub>2</sub> are known to undergo CuI-catalysed dehydrohalogenation reactions with

terminal alkynes in the presence of amine solvents (X = Cl [2,3,8,21–24,26,41,42,51,52]; I [11]) in keeping with these general observations, reaction of **3** with 4-ethynyl anisole or 4-ethynyl-*n*-phenylenedi-*p*-anisylamine (prepared from **2** by Sonogashira cross-coupling with trimethylsilylacetylene and subsequent desilylation) [53] in NHEt<sub>2</sub> and catalytic (ca. 15%) CuI gave the alkynyl complexes *trans*-Pt(C≡CAr)(C<sub>6</sub>H<sub>4</sub>NAr<sub>2</sub>)(PPh<sub>3</sub>)<sub>2</sub> (**4a**, 87%) and *trans*-Pt(C≡CC<sub>6</sub>H<sub>4</sub>NAr<sub>2</sub>)(C<sub>6</sub>H<sub>4</sub>NAr<sub>2</sub>)(PPh<sub>3</sub>)<sub>2</sub> (**4b**, 63%) as precipitates of analytical purity (Scheme 2). The acetylide ligand gave rise to a strong  $\nu(\text{C}\equiv\text{C})$  band at 2107 (**4a**) or 2105 (**4b**) cm<sup>-1</sup>, with whilst the *trans* geometry was again confirmed by the observation of a singlet in the <sup>31</sup>P NMR spectrum in each case (**4a** 20.84 ( $J_{\text{Pt-P}} = 2985$  Hz); **4b** 20.95 ( $J_{\text{Pt-P}} = 2981$  Hz)). The alkynyl carbons were not observed in the <sup>13</sup>C NMR spectra, with the weak signals from these quaternary carbons presumably being further reduced by coupling to both <sup>31</sup>P and <sup>195</sup>Pt. The chemically distinct OMe groups on both aryl and arylacetylide ligands were, however, readily observed in both <sup>1</sup>H and <sup>13</sup>C NMR spectra, and further confirm the presence of the alkynyl ligand.

In an entirely analogous manner, the CuI-catalysed reaction of two equivalents of **3** with 1,4-diethynyl benzene gave the bimetallic complex  $\{trans\text{-Pt}(\text{C}_6\text{H}_4\text{NAr}_2)(\text{PPh}_3)_2\}_2(\mu\text{-C}\equiv\text{C}\text{-}1,4\text{-C}_6\text{H}_4\text{C}\equiv\text{C})$  (**5**, 54%) whilst 3:1 stoichiometric reaction of **3** with redox-active tris(4-ethynylphenyl)amine gave trimetallic N{C<sub>6</sub>H<sub>4</sub>C≡CPt(C<sub>6</sub>H<sub>4</sub>NAr<sub>2</sub>)(PPh<sub>3</sub>)<sub>2</sub>}<sub>3</sub> (**6**, 67%) (Scheme 2). The identity of these multimetallic systems was also readily confirmed by multinuclear NMR and IR spectroscopies, MALDI-MS and elemental analysis, or in the case of **5**, ESI-HRMS. In addition to the observation of the [M]<sup>+</sup> (**5**) or



Scheme 1. The preparation of **1** and **2**.



Scheme 2. The preparation of **3**, **4a**, **4b**, **5** and **6**. (a) CuI (cat)/NHEt<sub>2</sub>/HC≡CC<sub>6</sub>H<sub>4</sub>R. (b) CuI (cat)/NHEt<sub>2</sub>/HC≡CC<sub>6</sub>H<sub>4</sub>C≡CH. (c) CuI (cat)/NHEt<sub>2</sub>/N(C<sub>6</sub>H<sub>4</sub>C≡CH-4)<sub>3</sub>.

$[M+H]^+$  (**6**) ions, the presence of the fully metallated bis- and tris-alkynyl ligands was confirmed by the observation of a single  $\nu(C\equiv C)$  band at 2103 (**5**) or 2105 (**6**)  $\text{cm}^{-1}$  and the absence of  $\nu(\equiv C-H)$  bands in the IR spectra of these complexes. The protons of the aryl rings of the bridging ligand were observed as a singlet (**5**: 5.72 ppm) or doublets (**6**: 5.93, 6.31 ppm;  $J_{\text{HH}} = 9$  Hz) whilst the other spectroscopic features were similar to those of the mono-metallic complexes **4a** and **4b**.

## 2.2. Molecular structures

Pale yellow crystals of **4a** (Fig. 1) and **4b** (Fig. 2) that were suitable for study by X-ray diffraction were grown by slow

diffusion of EtOH into a  $\text{CH}_2\text{Cl}_2$  solution of the compound. Selected bond lengths ( $\text{\AA}$ ), bond and torsion angles ( $^\circ$ ) are given in Table 1.

The molecular structures of **4a** and **4b** confirm the anticipated connectivity and *trans*-geometry of the complexes. The Pt centre displays the expected square-planar arrangement whilst the triarylamine fragments are arranged in the usual propeller-like geometry. [54–56] The greatest significant differences in the two structures arise in the alkyne fragment with some evidence for a degree of cumulenic character in the N2–C26···C22–C21 portion of **4b**, although the relatively low precision of the later structure prohibits detailed analysis. The Pt1–C21 bond in **4a** is slightly shorter than in **4b**, perhaps reflecting a greater degree of

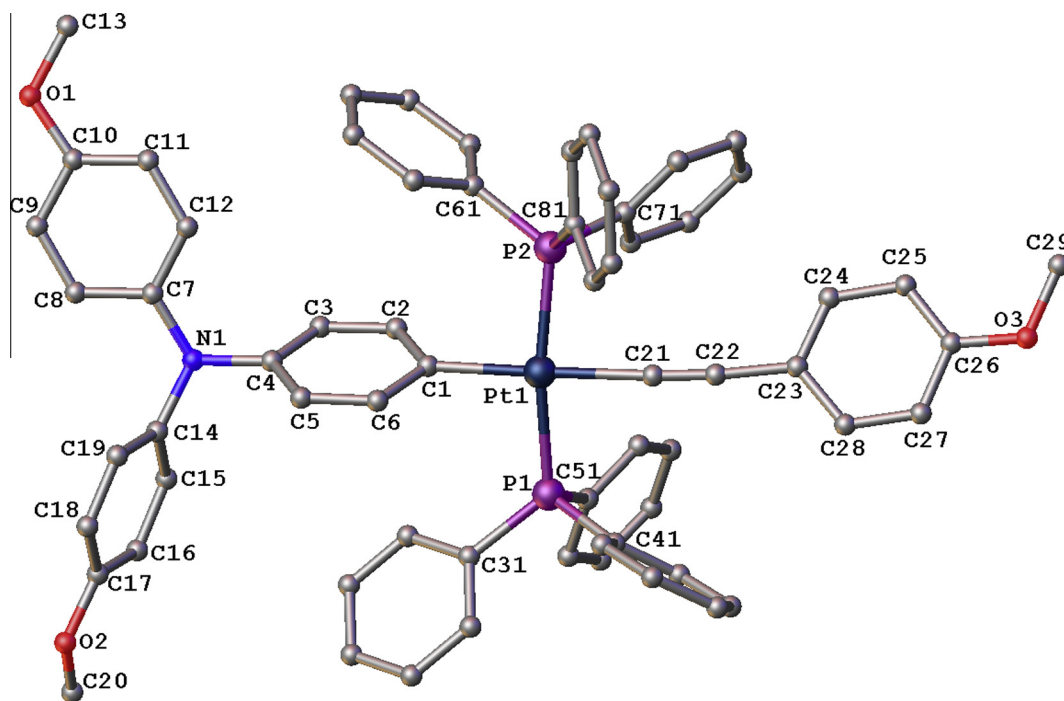


Fig. 1. A plot of a molecule of **4a** showing the atom labelling scheme, with thermal ellipsoids plotted at 50%. Hydrogen atoms have been omitted for clarity.

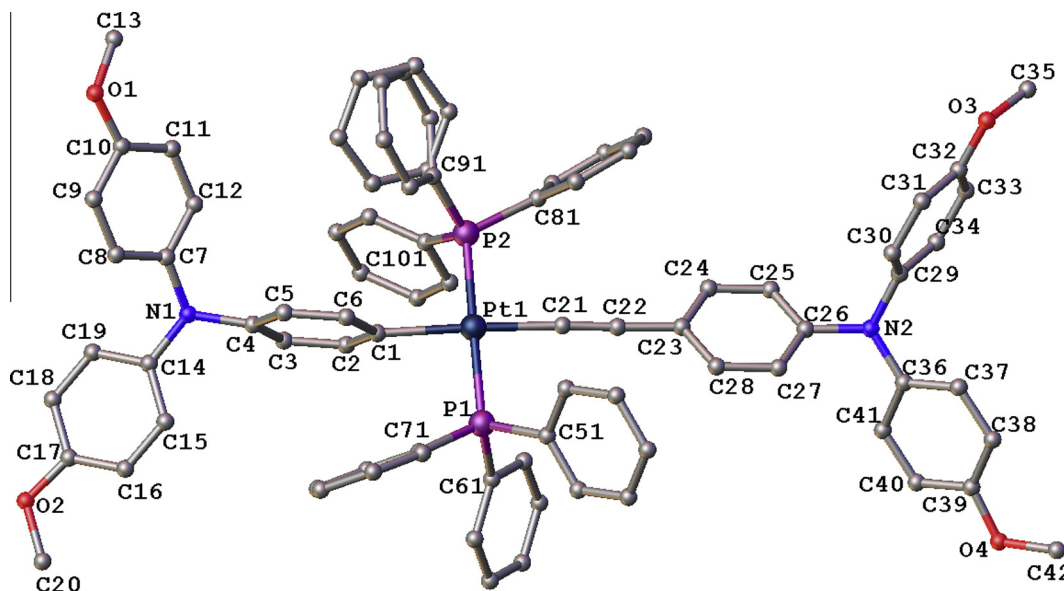


Fig. 2. A plot of a molecule of **4b** showing the atom labelling scheme, with thermal ellipsoids plotted at 50%. The disorder in the C91 ring is shown (see Experimental), and hydrogen atoms have been omitted for clarity.

electrostatic attraction between Pt1–C1 brought about by the electron donating OMe group at C26.

### 2.3. Electrochemical characterisation

The triarylamine moiety is a well-known organic electrophore [54–57] which features prominently in the design of organic hole-transporting materials [58] and mixed-valence compounds [44,46,59–61]. The presence of one or more triarylamine groups in compounds **4**–**6** prompted consideration of their electrochemical response. Cyclic voltammograms were recorded in  $\text{CH}_2\text{Cl}_2/0.1 \text{ M NBU}_4[\text{PF}_6]$  solutions at Pt microdot working electrodes, and referenced against an internal decamethylferrocene/decamethylferrocenium couple to ferrocene [62] (Fig. 3). In each case peak currents displayed a linear relationship with  $\nu^{1/2}$  (for scan rates  $\nu = 100, 200, 400, 800 \text{ mV s}^{-1}$ ), with peak current ratios  $0.98 < i_{\text{pa}}/i_{\text{pc}} < 1.0$ .

Taking **4a** as a model system, the presence of the  $\sigma$ -bonded Pt moiety results in less positive oxidation potential for the triarylamine moiety than in simpler organic derivatives [56]. The forward and reverse waves display a separation  $\Delta E_{\text{p}}(1)$  of 87 mV which is comparable to that of the internal  $\text{FcP}_2^*/[\text{FcP}_2^+]^+$  reference couple (84 mV) (Table 2). The introduction of a second, ethynyl substituted triarylamine in **4b** causes a small (+40 mV) shift in the half-wave potential of the metallated triarylamine (Table 2), with a second reversible wave arising from the ethynyl triarylamine at 189 mV. In the case of the bis(triarylamine) derivative **5**, only a single redox wave could be observed for the two equivalent triarylamine moieties, with the characteristics of a one-electron process pointing to the complete independence of these moieties through the  $\text{Pt}-\text{C}\equiv\text{C}_6\text{H}_4-\text{C}\equiv\text{C}-\text{Pt}$  chain. In keeping with this proposition, the voltametric wave shape was unchanged in the very weakly ion-pairing electrolyte  $\text{NBU}_4[\text{B}\{\text{C}_6\text{H}_3-3,5-(\text{CF}_3)_2\}_4]^-$  [63–66]. The electrochemical response

**Table 1**  
Selected bond lengths (Å), bond and torsion angles ( $^\circ$ ) for **4a** and **4b**.

	<b>4a</b>	<b>4b</b>		<b>4a</b>	<b>4b</b>
Pt1–P1	2.2944(7)	2.286(3)	C1–Pt1–C21	178.66(10)	176.6(3)
Pt1–P2	2.2892(7)	2.313(3)	P1–Pt1–P2	169.73(3)	175.48(10)
Pt1–C1	2.057(3)	2.144(5)	C1–Pt1–P1	94.14(7)	90.90(19)
Pt1–C21	2.072(3)	1.993(10)	C1–Pt1–P2	93.44(7)	89.88(19)
N1–C4	1.438(4)	1.464(9)	P1–Pt1–C21	87.20(7)	88.1(3)
N1–C7	1.415(4)	1.431(10)	P2–Pt1–C21	85.22(7)	90.8(3)
N1–C14	1.438(4)	1.418(9)			
C21–C22	1.138(4)	1.236(12)	C2–C1–C23–C24	41.49	55.48
C22–C23	1.479(4)	1.435(10)	C3–C4–C7–C8	120.47	144.59
N2–C26		1.457(8)	C3–C4–C14–C15	42.10	79.69
N2–C29		1.460(8)	C25–C26–C29–C30		101.11
N2–C36		1.414(9)	C25–C26–C36–C37		121.26

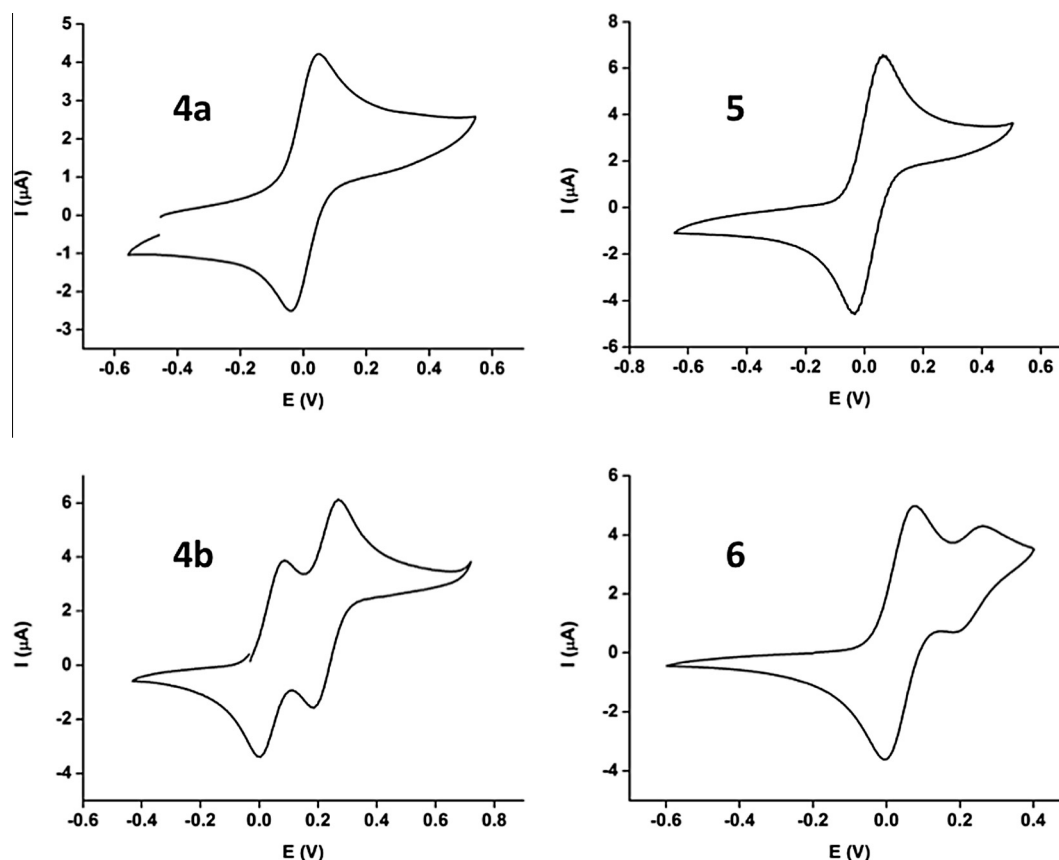


**Fig. 3.** Plots of the cyclic voltammograms of **4a**, **4b**, **5** and **6** in  $\text{CH}_2\text{Cl}_2$  with 0.1 M  $\text{NBU}_4[\text{PF}_6]$  at a scan rate of 100 mV/s and referenced against  $[\text{FcP}_2^*/\text{FcP}_2^+]^+$  at  $-0.48 \text{ V}$  vs  $\text{FcP}_2/[\text{FcP}_2]^+ + 0.0 \text{ V}$ .

of the branched molecule **6** was consistent with the points noted for the smaller analogues, with an initial oxidation event at +38 mV ( $\Delta E_p(1) = 80$  mV) being followed by a second process of 1/3rd the peak current at +204 mV ( $\Delta E_p(2) = 76$  mV). These processes can clearly be associate with the near simultaneous oxidation of the three external, metallated triarylamine moieties, and the internal tris(ethynyl)triarylamine core.

#### 2.4. Spectroelectrochemical investigations

To further explore the redox products derived from **4–6** a series of IR (Fig. 4, Table 3) and UV–Vis–NIR (Fig. 5, Fig. 6) spectroelectrochemical experiments were conducted. IR spectroelectrochemical investigations carried out with ca. 1 mM solutions in 0.1 M NBu<sub>4</sub> [PF<sub>6</sub>]/CH<sub>2</sub>Cl<sub>2</sub> show that the neutral complexes **4a**, **4b**, **5** and **6** all give rise to a single  $\nu(\text{C}\equiv\text{C})$  band near 2100 cm<sup>-1</sup> (Table 3), which provides a convenient spectroscopic marker for redox induced

structural changes in this series of compounds.[67] Oxidation of the reference compound **4a** to [4a]<sup>+</sup> results only a decrease in the intensity of the  $\nu(\text{C}\equiv\text{C})$  band, with no discernable change in frequency. An entirely analogous decrease in intensity with the most modest of shifts to higher wavenumber accompanies oxidation of **5** to [5]<sup>2+</sup>, which is consistent with the conclusions drawn from the electrochemical analysis concerning the independence of the amine sites.

In contrast, oxidation of **4b** to [4b]<sup>+</sup> results in both a small decrease in intensity of the initial  $\nu(\text{C}\equiv\text{C})$  band, together with the appearance of a broad, poorly structured  $\nu(\text{C}\equiv\text{C})$  band envelope between 2071–2027 cm<sup>-1</sup>. Further oxidation to [4b]<sup>2+</sup> results in a substantial increase in the intensity of this lower energy band envelope. These IR features are accompanied by the appearance of

**Table 2**

Oxidation potentials for platinum complexes **4–6** in CH<sub>2</sub>Cl<sub>2</sub> with 0.1 M NBu<sub>4</sub>[PF<sub>6</sub>] at a scan rate of 100 mV/s and referenced against [FeCp<sub>2</sub>/FeCp<sub>2</sub>]<sup>+</sup> at -0.48 V vs FeCp<sub>2</sub>/[FeCp<sub>2</sub>]<sup>+</sup> = +0.0 V.

Compound	$E_{1/2(1)}/\text{mV}$	$\Delta E_p(1)$	$E_{1/2(2)}/\text{mV}$	$\Delta E_p(2)$	$ E_2 - E_1 /\text{mV}$
<b>4a</b>	4	87			
<b>4b</b>	44	84	189	83	145
<b>5</b>	12	93			
<b>6</b>	38	80	204	76	166

**Table 3**

Summary of IR spectra from compounds [4–6]<sup>n+</sup> in their electrochemically accessible redox states.

Compound	$n = 0$	$n = 1$	$n = 2$
[4a] <sup>n+</sup>	2107(s)	2107(m)	
[4b] <sup>n+</sup>	2105(s)	2105(m) 2071(s) 2052(sh) 2027(sh)	2071(vs) 2052(sh) 2027(sh)
[5] <sup>n+</sup>	2103(s) $n = 0$	$n = 3$	2105(m) $n = 4$
[6] <sup>n+</sup>	2105(s)	2107(m)	2068(s) 2027(sh)

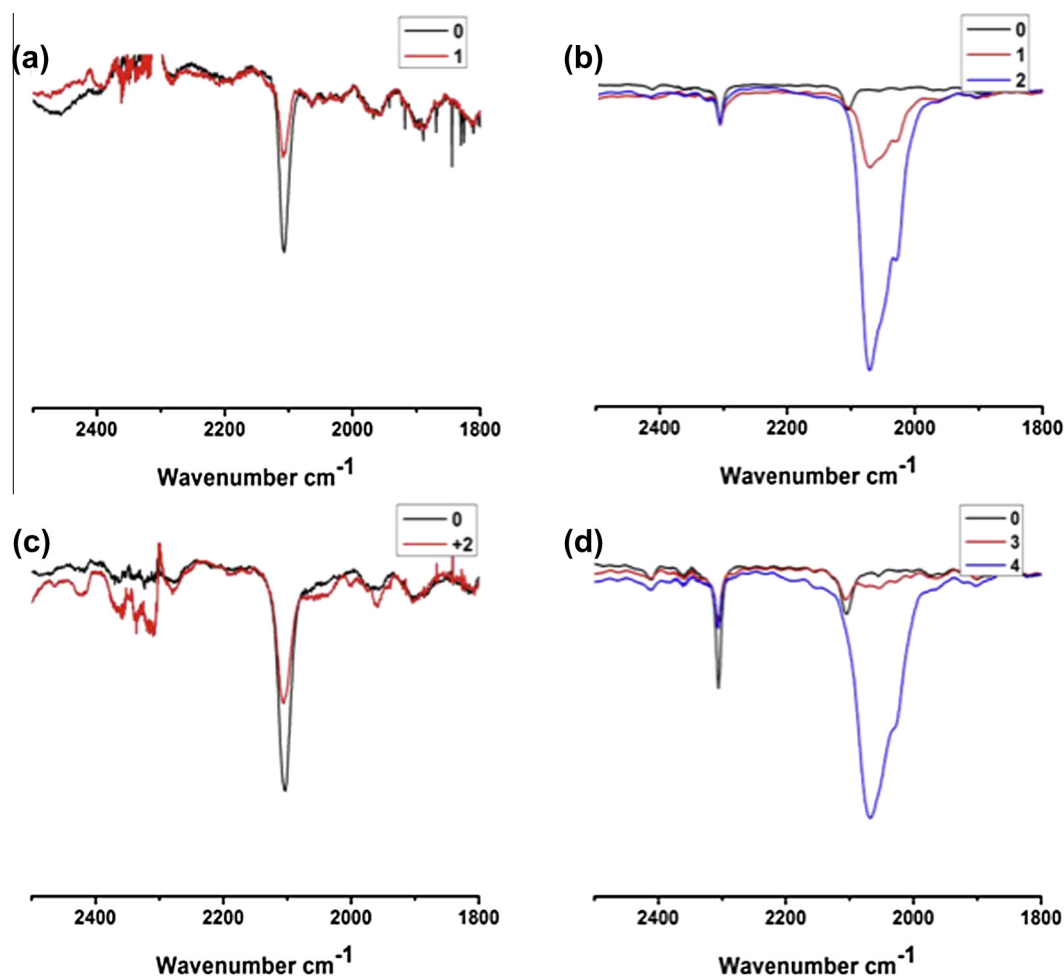


**Fig. 4.** IR spectra of (a) [4a]<sup>n+</sup>, (b) [4b]<sup>n+</sup>, (c) [5]<sup>n+</sup> and (d) [6]<sup>n+</sup> showing the  $\nu(\text{C}\equiv\text{C})$  band in the various oxidation states generated by *in situ* electrochemical oxidation in CH<sub>2</sub>Cl<sub>2</sub>/0.1 M NBu<sub>4</sub>PF<sub>6</sub> in an OTTE cell.

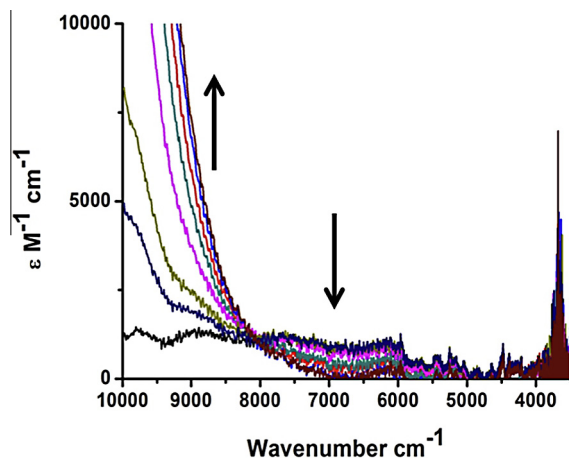


Fig. 5. An expansion of the NIR region of  $[4b]^+$  on oxidation to  $[4b]^{2+}$  showing the collapse of the IVCT band.

a weak NIR band unique to  $[4b]^+$  with an apparent band centre at  $8000\text{ cm}^{-1}$ , which collapses on oxidation to  $[4b]^{2+}$  (Fig. 4) and therefore suggestive of  $\{\text{Ar}_2\text{NC}_6\text{H}_4\text{C}\equiv\text{C}\} \rightarrow \{\text{PtC}_6\text{H}_4\text{N}^+\text{Ar}_2\}$  IVCT character and hence description of  $[4b]^+$  as a weakly coupled mixed-valence complex (rudimentary analysis of the NIR band using the Hush expressions and taking the crystallographically determined N1–N2 distance as a proxy for the electron-transfer distance gives  $H_{ab} = 170\text{ cm}^{-1}$ ).

Similarly, initial three-electron oxidation of **6** to  $[6]^{3+}$  gives the same pattern of behaviour, with oxidation accompanied by a decrease in intensity of the  $\nu(\text{C}\equiv\text{C})$  band and a subtle shift to higher wavenumbers, but now with a weaker  $\nu(\text{C}\equiv\text{C})$  band envelope at lower wavenumbers, together with a NIR band ( $\nu_{\text{max}} = 8700\text{ cm}^{-1}$ ) of now appreciable intensity. However, further oxidation to  $[6]^{4+}$  results in the NIR region being masked by the tail of a higher energy optical band. Nevertheless, assuming the NIR feature in  $[6]^{3+}$  is due to an IVCT-like transition, a  $H_{ab}$  value of ca.  $130\text{ cm}^{-1}$  (allowing for the three possible transitions) is obtained. The  $\nu(\text{C}\equiv\text{C})$  IR band envelope of  $[6]^{4+}$  is similar to that of the linear

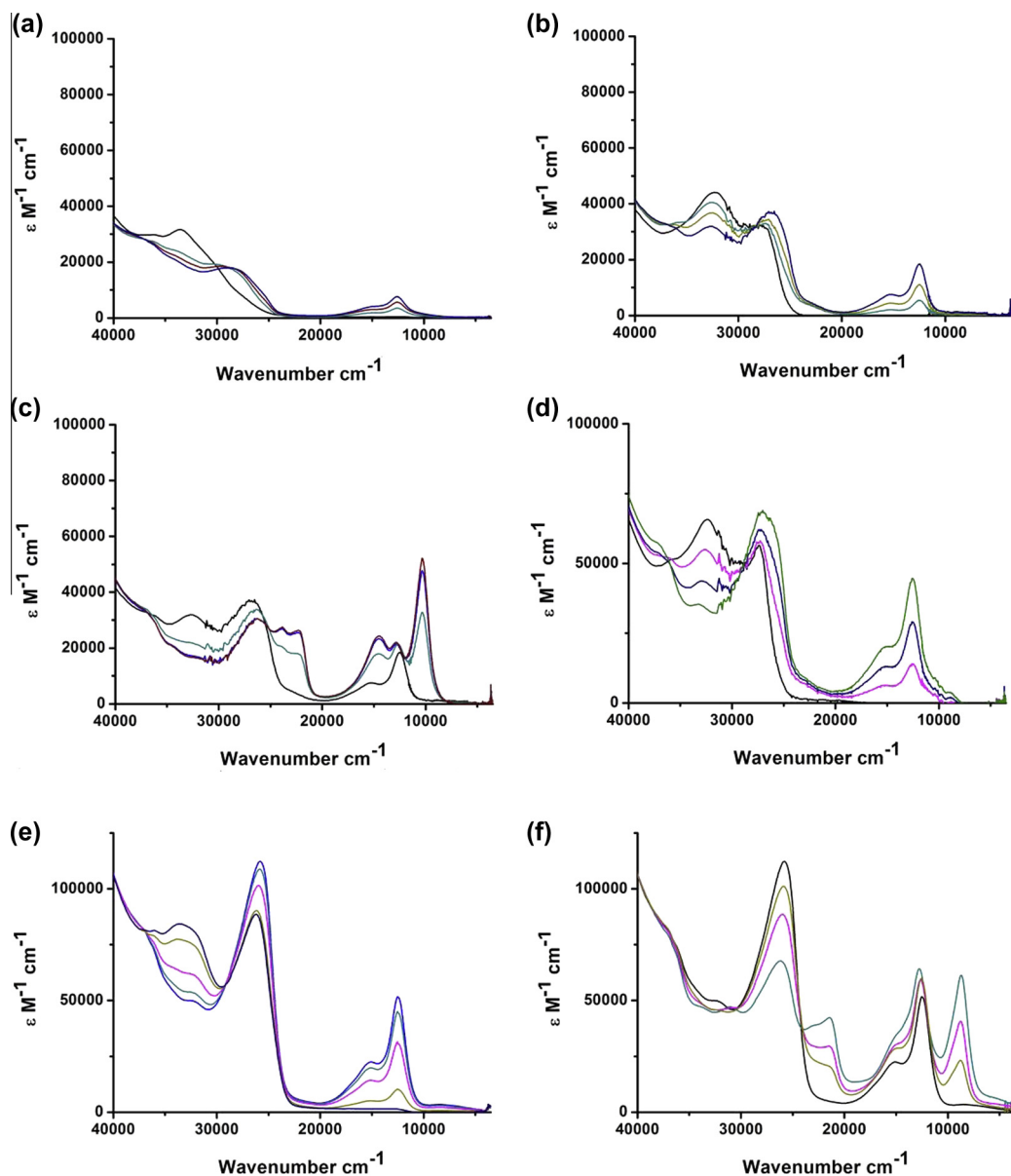


Fig. 6. UV-Vis-NIR spectra of (a)  $[4a] \rightarrow [4a]^+$ , (b)  $[4b] \rightarrow [4b]^+$ , (c)  $[4b]^+ \rightarrow [4b]^{2+}$ , (d)  $[5] \rightarrow [5]^{2+}$ , (e)  $[6] \rightarrow [6]^{3+}$  and (f)  $[6]^{3+} \rightarrow [6]^{4+}$  showing the changes in the various oxidation states generated by *in situ* electrochemical oxidation in  $\text{CH}_2\text{Cl}_2/0.1\text{ M NBU}_4\text{PF}_6$  in an OTTL cell.

model **[4b]<sup>2+</sup>**. The observation of multiple  $\nu(\text{C}\equiv\text{C})$  features in these highly charged systems could be a result of Fermi coupling, as often observed by Lapinte in studies of open-shell iron complexes [68], or may arise from contributions to the spectral profile from multiple conformers [69,70].

To complement the IR spectra and to further investigate the electronic structures of these complexes, UV–Vis–NIR spectroelectrochemical studies of **4a**, **4b**, **5** and **6** were undertaken from ca. 1 mM solutions in 0.1 M NBu<sub>4</sub>PF<sub>6</sub>/CH<sub>2</sub>Cl<sub>2</sub> (Fig. 6). The complexes **4–6** all feature similar electronic absorption spectra with bands near 33 000 cm<sup>-1</sup> and 25 000 cm<sup>-1</sup>, arising from the two N → π\* transitions commonly observed in triarylamine complexes of general form NArAr'<sub>2</sub> (Fig. 6). [54–57]. As a result of the first oxidation events, in each case this band envelope is shifted somewhat to lower energy, with a new band envelope between 20 000–10 000 cm<sup>-1</sup> characteristic of an {NArAr'<sub>2</sub>}<sup>+</sup> fragment and arising from π → N<sup>+</sup> transitions, possibly admixed with some Pt → N<sup>+</sup> character in these cases [46], in addition to the low energy IVCT bands noted earlier for **[4b]<sup>+</sup>** and **[6]<sup>3+</sup>**. Further oxidation of the complexes **[4b]<sup>+</sup>** to **[4b]<sup>2+</sup>**, and **[6]<sup>3+</sup>** to **[6]<sup>4+</sup>** resulted in a collapse of the IVCT feature (more clearly evident in the case of **[4b]<sup>+</sup>** → **[4b]<sup>2+</sup>**) and the appearance of a second set of π → N<sup>+</sup>/Pt → N<sup>+</sup> bands at lower energy.

### 2.5. Quantum chemical calculations

To complete the description of these redox-active Pt-ethynyl/triarylamine assemblies, we turned to quantum-chemical calculations using the BLYP35 functional and COSMO (dichloromethane) solvent model. The combination of a high amount of direct exchange in the functional and the inclusion of a solvent model has been shown to allow the accurate description of charge localization/delocalization now in a wide range of organic and organometallic mixed-valence complexes spanning the weakly to strongly coupled regime.

As expected, complexes **[4a]<sup>+</sup>** and **[4b]<sup>+</sup>** exhibit spin densities localised at one triarylamine unit in their monocationic forms, and in the case of **[4b]<sup>+</sup>** this localization takes place at the triarylamine moiety which is directly connected to the platinum (Fig. 7). This amine-localised redox behaviour is in agreement with previous studies of platinum-bridged mixed-valent triarylamine systems. Vibrational analysis within a harmonic framework provides excellent agreement between the computed  $\nu(\text{C}\equiv\text{C})$  frequency at 2075 cm<sup>-1</sup> and the experimental at 2071 cm<sup>-1</sup> for **[4b]<sup>+</sup>** after scaling by an empirical factor of 0.95. In contrast for **[4a]<sup>+</sup>** no intensity is calculated for  $\nu(\text{C}\equiv\text{C})$ , as the ethynyl-unit is not involved in the redox event, consistent with the decrease in intensity of this band observed experimentally.

To characterise the UV–Vis–NIR transitions we turned to TDDFT calculations employing the same BLYP35/COSMO(CH<sub>2</sub>Cl<sub>2</sub>) combination as for the ground-state analysis. We note in passing that despite the elaborately discussed failure of TDDFT in describing charge transfer excitations, this quantum-chemical approach has proven to yield reliable results for Class II systems [71]. All complexes exhibit localised charge distributions in the ground-state, and the reasonable agreement between experimental bands and calculated excitations is consistent with previous observations at this level for Class II systems. A recently published study has extensively discussed the general electronic and spectroscopic features of platinum alkynyl complexes featuring triarylamine redox centres [46]. We therefore refrain from a detailed discussion of **[4a]<sup>+</sup>** and **[4b]<sup>+</sup>**. We note simply that these two complexes exhibit a typical β-HOMO–β-SOMO transition at 9996 cm<sup>-1</sup> (**[4a]<sup>+</sup>**, exp. ca. 10 000 cm<sup>-1</sup>), and at 6514 cm<sup>-1</sup> (**[4b]<sup>+</sup>**, exp. ca. 7000 cm<sup>-1</sup>), respectively. These transitions arise from charge transfer between the alkynyl ligand and its substituent to the oxidised triarylamine

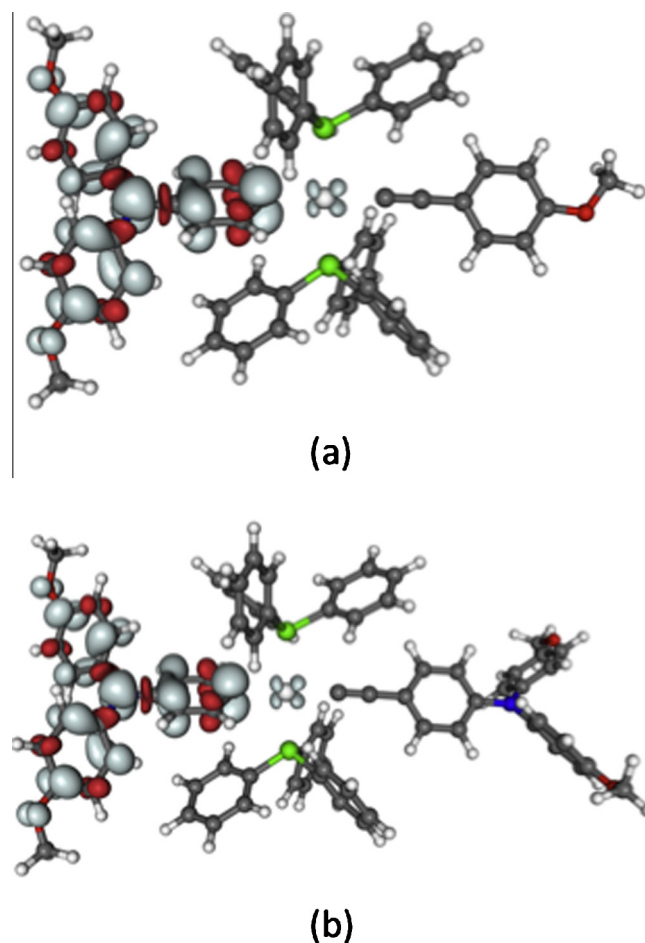


Fig. 7. Plots of the spin density in (a) **[4a]<sup>+</sup>** and (b) **[4b]<sup>+</sup>**.

moiety directly coordinated to Pt. At higher energies characteristic excitations associated with the oxidised triarylamine unit and MLCT transitions are computed (see SI). Interestingly the ethynyl unit contributes more to the orbitals involved in the excitations for **[4a]<sup>+</sup>** than **[4b]<sup>+</sup>** (see SI).

Although **[5]<sup>+</sup>** was not sufficiently thermodynamically stable to be observed in the spectroelectrochemical experiments, some information concerning this unusual mixed-valence complex can be obtained from quantum chemical calculations using a truncated model {*trans*-Pt(C<sub>6</sub>H<sub>4</sub>NAr<sub>2</sub>)(PMe<sub>3</sub>)<sub>2</sub>}(μ-C≡C-1,4-C<sub>6</sub>H<sub>4</sub>C≡C) (**[5-Me]<sup>+</sup>**). The compound **[5-Me]<sup>+</sup>** is calculated to exhibit a N → N<sup>+</sup> IVCT transition at 6692 cm<sup>-1</sup> with only modest intensity ( $\mu_{\text{trans}} = 0.8$  D) as expected for a weakly coupled system. The β-HOMO–1 – β-SOMO charge-transfer excitation at 9808 cm<sup>-1</sup> ( $\mu_{\text{trans}} = 3.8$  D) from the oxidised triarylamine moiety to the diethynylbenzene bridge is responsible for the next lowest-energy excitation (Fig. 8). The two most intense transitions are computed at 14,966 cm<sup>-1</sup> ( $\mu_{\text{trans}} = 7.4$  D) and 16 258 cm<sup>-1</sup> ( $\mu_{\text{trans}} = 5.5$  D) as is commonly observed for oxidised triarylamine compounds. The first corresponds to a π → N<sup>+</sup> CT excitation with one triarylamine unit (43%), the neighbouring platinum (20%) and the diethynylbenzene (19%) contributing significantly to the π-type orbital. The second excitation is best described in terms of an IC excitation at the charged triarylamine.

For **[5-Me]<sup>2+</sup>**, which was observed in the spectroelectrochemical experiments (Fig. 5d), the calculations provide almost degenerate broken-symmetry (BS, “open-shell singlet”) and triplet state, with the former being slightly lower with spin-density distribution illustrated in Fig. 9. Given that hybrid functionals with increased exact exchange admixture tend to favour high-spin states, the negligible energy difference of only 0.04 kJ/mol (calculated using

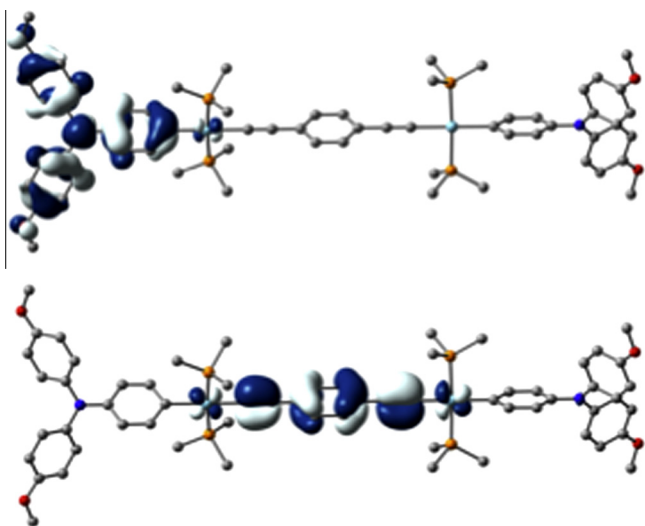


Fig. 8. Isosurface plots ( $\pm 0.03$  a.u.) of the  $\beta$ -SOMO (top) and  $\beta$ -HOMO-1 (bottom) of  $[5\text{-Me}]^+$ . Hydrogen atoms have been omitted for clarity.

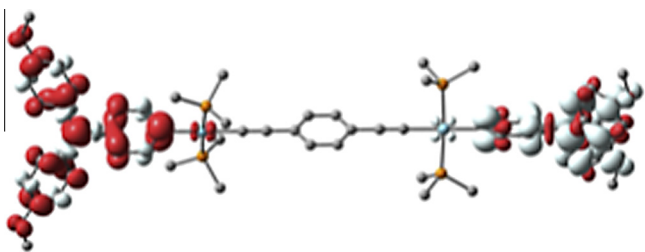


Fig. 9. Spin density isosurface plot ( $\pm 0.002$  a.u.) of the (broken-symmetry) low-spin state of  $[5\text{-Me}]^{2+}$ . Hydrogen atoms have been omitted for clarity.

the Yamaguchi spin projection procedure) in combination with the onset of spin-contamination ( $\langle S^2 \rangle_{\text{singlet}} = 1.06$ ) indicate that both states likely contribute significantly to the spectra. But as expected, the two spin states exhibit very similar spectral features both in the ground- (e.g.  $\nu(\text{C}\equiv\text{C})_{\text{singlet}} = 2124 \text{ cm}^{-1}$  and  $\nu(\text{C}\equiv\text{C})_{\text{triplet}} = 2124 \text{ cm}^{-1}$ ) and the excited state. TDDFT gives very similar transition energies for the BS (e.g.  $11057 \text{ cm}^{-1}$ ,  $\mu_{\text{trans}} = 5.9 \text{ D}$ ) and triplet state (e.g.  $11073 \text{ cm}^{-1}$ ,  $\mu_{\text{trans}} = 6.1 \text{ D}$ ), which likely correspond to the low energy shoulder observed near  $10000 \text{ cm}^{-1}$  (Fig. 6d). But while excitations arise mainly from and to  $\alpha$ -orbitals for the BS state, transitions involve almost exclusively  $\beta$ -orbitals for the triplet. The lowest-energy transition arises in both cases from orbitals located at the diethynylbenzene unit. But while the charge is transferred upon excitation from one triarylamine in the case of the BS state, both triarylamine moieties contribute significantly (30% and 41%) to the orbital involved in the transition for the triplet.

With this background understanding of the spectroscopic features of the smaller model complexes  $[4\mathbf{a}]^+$ ,  $[4\mathbf{b}]^+$  and the calculated results from  $[5\text{-Me}]^+$  and  $[5\text{-Me}]^{2+}$  it is possible to readily assign the spectroscopic features in the larger systems  $[6]^{3+}$  and  $[6]^{4+}$ . The observation of the characteristic intense triarylamine bands between  $10000\text{--}20000 \text{ cm}^{-1}$  together with the current ratios described in the electrochemistry section are consistent with the oxidation of the peripheral amine moieties in  $[6]^{3+}$ , with the less intense NIR feature at  $5500 \text{ cm}^{-1}$  arising from IVCT like processes from the inner to outer amines, all of which are similar to the analogous transitions in  $[4\mathbf{b}]^+$ . Further oxidation of the central amine moiety in  $[6]^{4+}$  gives rise to a second set of amine based transitions similar to those observed in  $[4\mathbf{b}]^{2+}$ .

### 3. Conclusion

The synthesis of mono-ethynyl platinum species with redox active triarylamine ligands, **4a**, **4b**, **5** and **6**, has successfully been achieved through the oxidative addition of the triarylamine iodide with the platinum precursor  $\text{Pt}(\text{PPh}_3)_4$  and then  $\text{CuI}$ -catalysed coupling to the respective 1-alkyne. These compounds have been studied electrochemically and spectroelectrochemically, revealing weak interactions between the amine electrophores when bridged by the  $\{-\text{Pt}(\text{C}\equiv\text{C})(\text{PPh}_3)_2\}$  moiety.

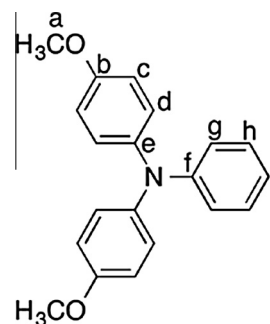
### 4. Experimental

#### 4.1. Synthesis

All reactions were carried out under an atmosphere of nitrogen using standard Schlenk techniques as a matter of routine, although no special precautions were taken to exclude air or moisture during work-up. Reaction solvents were purified and dried using an Innovative Technology SPS-400, and degassed before use, but no special precautions were taken during work up, isolation or crystallisation. The compounds 4-ethynylphenylenedi-*p*-anisylamine [53],  $\text{Pt}(\text{PPh}_3)_4$  [50] and  $\text{Pd}(\text{PPh}_3)_4$  [72] were prepared by the literature methods.

NMR spectra were recorded on a Bruker Avance ( $^1\text{H}$  400.13 MHz,  $^{13}\text{C}$  100.61 MHz,  $^{31}\text{P}$  161.98 MHz) spectrometer from  $\text{CDCl}_3$  solutions unless otherwise indicated, and referenced against solvent resonances ( $\text{CDCl}_3$   $^1\text{H}$  7.26  $^{13}\text{C}$  77.0). IR spectra ( $\text{CH}_2\text{Cl}_2$ ) were recorded using a Nicolet 6700 spectrometer from cells fitted with  $\text{CaF}_2$  windows. Electrospray ionisation mass spectra were recorded using Thermo Quest Finnigan Trace MS-Trace GC or WATERS Micro-mass LCT spectrometers. Samples in dichloromethane (1 mg/mL) were 100 times diluted in either methanol or acetonitrile, and analysed with source and desolvation temperatures of  $120 \text{ }^\circ\text{C}$ , with cone voltage of 30 V. ASAP mass spectra were recorded from solid aliquots on LCT Premier XE mass spectrometer (Waters Ltd, UK) or Xevo QTOF mass spectrometer (Waters Ltd, UK) in which the aliquot is vaporised using hot  $\text{N}_2$ , ionised by a corona discharge and carried to the TOF detector (working range  $100\text{--}1000 \text{ m/z}$ ).

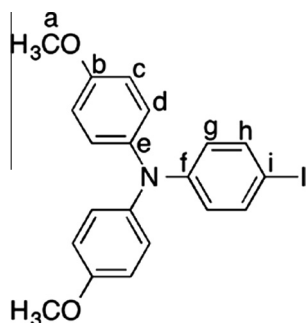
#### 4.1.1. Synthesis of $N(\text{C}_6\text{H}_5)(\text{C}_6\text{H}_4\text{OMe-4})_2$ (**1**) [47]



An oven dried Schlenk flask was charged with *o*-xylene (30 mL) and the solvent degassed. To this solution, 4-iodoanisole (15.00 g, 64.1 mmol),  $\text{CuCl}$  (0.201 g, 2.03 mmol), 1,10-phenanthroline (0.274 g, 1.5 mmol) and aniline (2.78 mL, 30.5 mmol) were added, the mixture was heated at reflux for 35 min,  $\text{KOH}$  (13.70 g, 244 mmol) was added and the mixture heated at reflux for 28 h, cooled, poured into  $\text{H}_2\text{O}$  (150 mL) and extracted with  $\text{CH}_2\text{Cl}_2$  ( $3 \times 60 \text{ mL}$ ). The organic layers were combined and dried over  $\text{MgSO}_4$ , filtered and the solvent removed in vacuo. The residue was suspended in hexane and purified by silica column chromatography eluting with hexane increasing to hexane: $\text{CH}_2\text{Cl}_2$  (50:50), removal of the solvent and crystallisation from hot hexane gives the title

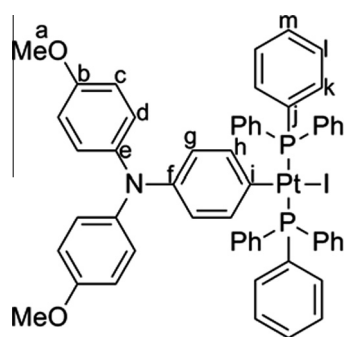
compound as a white solid. Yield 3.29 g, 32%.  $^1\text{H}$  NMR (400 MHz,  $\text{CDCl}_3$ )  $\delta$  7.16 (d,  $J = 7$  Hz, 2H), 7.05 (d,  $J = 9$  Hz, 4H), 6.94 (d,  $J = 7$  Hz, 2H), 6.90–6.85 (m, 1H), 6.82 (d,  $J = 9$  Hz, 4H), 3.80 (s, 6H). Literature:[47]  $^1\text{H}$  NMR ( $\text{CDCl}_3$ ):  $\delta = 7.25$ – $6.79$  (m, 13H, Ar), 3.79 ppm (s, 6H, OCH<sub>3</sub>). ESI-MS: 305.6 [ $\text{M}$ ]<sup>+</sup>.

#### 4.1.2. Synthesis of $N(\text{C}_6\text{H}_4\text{-}4)\text{Ar}_2$ (**2**) [73]



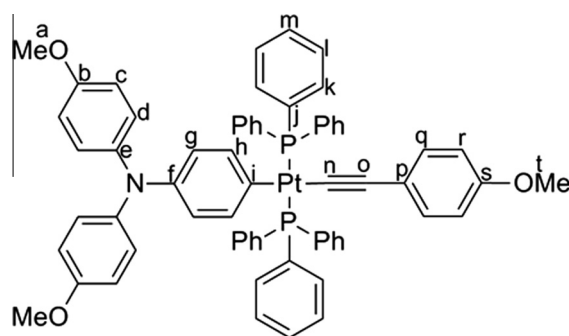
An oven dried Schlenk flask was charged with chloroform (90 mL) and the solvent degassed. To this solution, **1** (3.00 g, 9.8 mmol) and NIS (2.430 g, 10.8 mmol) were added with the exclusion of light followed by acetic acid (60 mL) and the mixture stirred at room temperature for 30 h and quenched with aqueous sodium thiosulphate (300 mg in 30 mL  $\text{H}_2\text{O}$ ) and extracted with  $\text{CH}_2\text{Cl}_2$  ( $3 \times 30$  mL). The organic layers were combined and dried over  $\text{MgSO}_4$ , filtered and the solvent removed in vacuo to give an off-white solid. Yield 3.14 g, 75%.  $^1\text{H}$  NMR (400 MHz,  $\text{CDCl}_3$ )  $\delta$  7.40 (d,  $J = 8$  Hz, 2H), 7.02 (d,  $J = 8$  Hz, 4H), 6.82 (d,  $J = 8$  Hz, 4H), 6.67 (d,  $J = 8$  Hz, 2H), 3.79 (s, 6H). Literature:  $^1\text{H}$  NMR (250 MHz,  $\text{CDCl}_3$ ):  $\delta$  7.40/6.67 (m, AA', 2 H/m, BB', 2H; I-C<sub>6</sub>H<sub>4</sub>), 7.03/6.82 (m, AA' ± BB', 8H;  $\text{H}_3\text{CO}$ -C<sub>6</sub>H<sub>4</sub>), 3.79 (s, 6H; MeO) ESI-MS: 431.5 [ $\text{M}$ ]<sup>+</sup>.

#### 4.1.3. Synthesis of $\text{trans-Pt}(\text{C}_6\text{H}_4\text{NAr}_2)(\text{PPh}_3)_2$ (**3**)



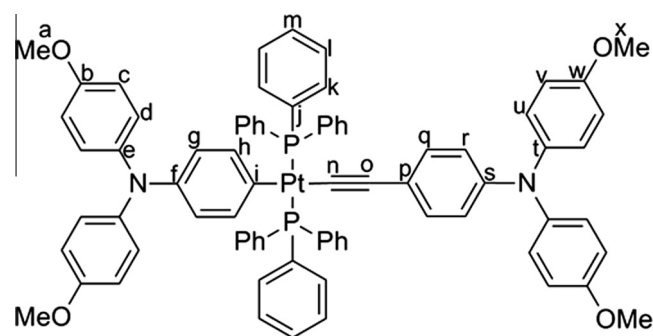
An oven dried Schlenk flask was charged with dry toluene (20  $\text{cm}^3$ ) and the solvent degassed. To this solution,  $\text{Pt}(\text{PPh}_3)_4$  (1.00 g, 0.804 mmol) and 4-iodophenylene-*p*-dianisylamine (0.693 g, 1.60 mmol) were added and the mixture stirred for 16 h at reflux. The mixture was cooled to ambient temperature and added to vigorously stirred hexane (150  $\text{cm}^3$ ) and the off-white precipitate was filtered and washed with hexane ( $2 \times 10$  mL). Yield 880 mg, 95%.  $^1\text{H}$  NMR ( $\text{CD}_2\text{Cl}_2$ )  $\delta$  3.76 (s, 6H, Ha), 5.98 (d,  $J = 8$  Hz, 2H, Hh), 6.71 (m, 10H, Hc,d and g), 7.34 (vt,  $J = 8$  Hz, 12H, Hk), 7.41 (t,  $J = 8$  Hz, 6H, Hm), 7.62 (m, 12H, Hl).  $^{31}\text{P}$  NMR ( $\text{CD}_2\text{Cl}_2$ ): 20.67 ( $J_{\text{Pt-P}} = 3074$  Hz).  $^{13}\text{C}$  NMR ( $\text{CD}_2\text{Cl}_2$ ): 154.72 (Cb, s), 142.22 (Ce, s), 141.78 (Cf, s), 136.17 (Cg, s), 135.08 (Cl, t,  $J_{\text{C-P}} = 5$  Hz), 131.80 (Cj, t,  $J_{\text{C-P}} = 28$  Hz), 129.88 (Cm, s), 127.58 (Ck, t,  $J_{\text{C-P}} = 5$  Hz), 125.19 (Cc, s), 122.99 (Ch, s), 113.99 (Cd, s), 55.39 (Ca, s). MALDI-MS(+)  $m/z$ : 1151.1 [ $\text{M}+\text{H}$ ]<sup>+</sup>. Anal. Calc. for: C, 58.44; H, 4.20; N, 1.22. Found: C, 58.60; H, 4.04; N, 1.29%.

#### 4.1.4. Synthesis of $\text{trans-Pt}(\text{C}\equiv\text{CAr})(\text{C}_6\text{H}_4\text{NAr}_2)(\text{PPh}_3)_2$ (**4a**)



An oven dried Schlenk flask was charged with dry  $\text{HNET}_2$  (10  $\text{cm}^3$ ) and the solvent degassed. To this solution, 4-ethynylanisole (0.017 g, 0.13 mmol), **3** (150 mg, 0.13 mmol) and  $\text{CuI}$  (4 mg) were added and the solution stirred at room temperature for 17 h. The precipitate was filtered, washed with ethanol ( $3 \times 5$   $\text{cm}^3$ ) and methanol ( $3 \times 5$   $\text{cm}^3$ ) and dried under airflow for 1 h. Yield 131 mg, 87%.  $^1\text{H}$  NMR ( $\text{CD}_2\text{Cl}_2$ ):  $\delta$  3.64 (s, 3H, Ht), 3.76 (s, 6H, Ha), 6.11 (d,  $J = 8$  Hz, 2H, Hh), 6.15 (d,  $J = 9$  Hz, 6H, Hr), 6.43 (d,  $J = 9$  Hz, 2H, Hq), 6.71 (d,  $J = 8$  Hz, 2H, Hg), 6.73 (m, 8H, Hc and d), 7.32 (vt,  $J = 8$  Hz, 12H, Hk), 7.40 (t,  $J = 8$  Hz, 6H, Hm), 7.64 (m, 12H, Hl).  $^{31}\text{P}$  NMR ( $\text{CD}_2\text{Cl}_2$ ): 20.84 ( $J_{\text{Pt-P}} = 2985$  Hz).  $^{13}\text{C}$  NMR ( $\text{CD}_2\text{Cl}_2$ ): 156.77 (Cs, s), 154.29 (Cb, s), 142.31 (Ce, s), 141.55 (Cf, s), 139.55 (Cg, s), 134.84 (Cl, t,  $J_{\text{C-P}} = 5$  Hz), 131.79 (Cj, t,  $J_{\text{C-P}} = 28$  Hz), 131.35 (Cq, s), 129.75 (Cm, s), 127.58 (Ck, t,  $J_{\text{C-P}} = 5$  Hz), 124.10 (Cc, s), 123.94 (Ch, s), 121.74 (Cp, s), 113.92 (Cd, s), 112.71 (Cr, s), 55.40 (Ca, s), 54.96 (Ct, s). MALDI-MS(+)  $m/z$ : 1155.3 [ $\text{M}+\text{H}$ ]<sup>+</sup>. IR ( $\text{CH}_2\text{Cl}_2$ )  $\nu(\text{C}\equiv\text{C})$  2107  $\text{cm}^{-1}$ . Anal. Calc. for: C, 67.58; H, 4.80; N, 1.21. Found: C, 67.45; H, 4.74; N, 1.17%.

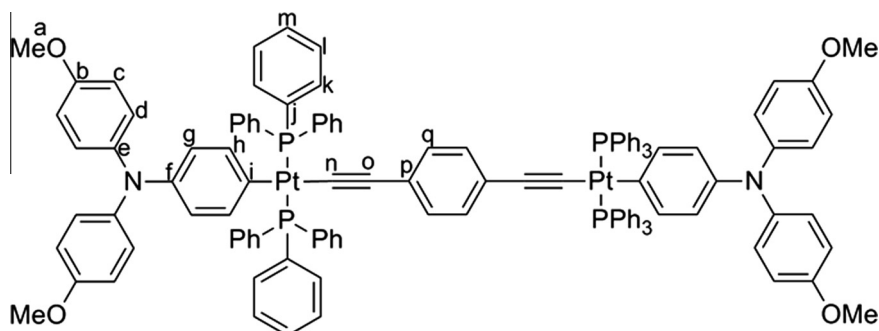
#### 4.1.5. Synthesis of $\text{trans-Pt}(\text{C}\equiv\text{CC}_6\text{H}_4\text{NAr}_2)(\text{C}_6\text{H}_4\text{NAr}_2)(\text{PPh}_3)_2$ (**4b**)



An oven dried Schlenk flask was charged with 4-ethynylene-*p*-anisylamine (0.043 g, 0.13 mmol) in dry  $\text{CH}_2\text{Cl}_2$  and the solvent removed *in vacuo*. Dry  $\text{HNET}_2$  (10  $\text{cm}^3$ ) was added and the solvent degassed. To this solution,  $\text{Pt}(\text{C}_6\text{H}_4\text{N}(\text{C}_6\text{H}_4\text{OCH}_3)_2)(\text{PPh}_3)_2$  (150 mg, 0.130 mmol) and  $\text{CuI}$  (4 mg) were added and the solution stirred at room temperature for 2 h. The precipitate was filtered, washed with methanol ( $3 \times 5$   $\text{cm}^3$ ), ethanol ( $3 \times 5$   $\text{cm}^3$ ) and hexane ( $3 \times 5$   $\text{cm}^3$ ) and dried under airflow for 1 h. Yield 109 mg, 63%.  $^1\text{H}$  NMR ( $\text{CD}_2\text{Cl}_2$ ):  $\delta$  3.76 (s, 12H, Ha and x), 6.03 (d,  $J = 8$  Hz, 2H, Hq), 6.11 (d,  $J = 8$  Hz, 2H, Hh), 6.44 (d,  $J = 8$  Hz, 2H, Hr), 6.68 (d,  $J = 8$  Hz, 2H, Hg), 6.73 (m, 8H, Hc and d), 6.76 (d,  $J = 8$  Hz, 4H, Hv), 6.89 (d,  $J = 8$  Hz, 4H, Hu), 7.32 (vt,  $J = 8$  Hz, 12H, Hk), 7.39 (t,  $J = 8$  Hz, 6H, Hm), 7.64 (m, 12H, Hl).  $^{31}\text{P}$  NMR ( $\text{CD}_2\text{Cl}_2$ ): 20.95 ( $J_{\text{Pt-P}} = 2981$  Hz).  $^{13}\text{C}$  NMR ( $\text{CD}_2\text{Cl}_2$ ): 155.48 (Cw, s), 154.29 (Cb, s), 145.33 (Ct, s), 142.31 (Ce, s), 141.59 (Cf, s), 141.12 (Cs, s), 139.53 (Cg, s), 134.84 (Cl, t,  $J_{\text{C-P}} = 5$  Hz), 131.781 (Cj,

t,  $J_{C-P} = 28$  Hz), 130.97 (Cq, s), 129.76 (Cm, s), 127.59 (Ck, t,  $J_{C-P} = 5$  Hz), 125.86 (Cu, s), 124.11 (Cc, s), 123.93 (Ch, s), 120.45 (Cr, s), 114.37 (Cv, s), 113.92 (Cd, s), 55.40 (Ca, s), 55.36 (Cx, s). MALDI-MS(+)  $m/z$ : 1352.3 [M+H]<sup>+</sup>. IR (CH<sub>2</sub>Cl<sub>2</sub>)  $\nu(C\equiv C)$  2105 cm<sup>-1</sup>. Anal. Calc. for: C, 69.27; H, 4.92; N, 2.07. Found: C, 69.05; H, 4.84; N, 2.11%.

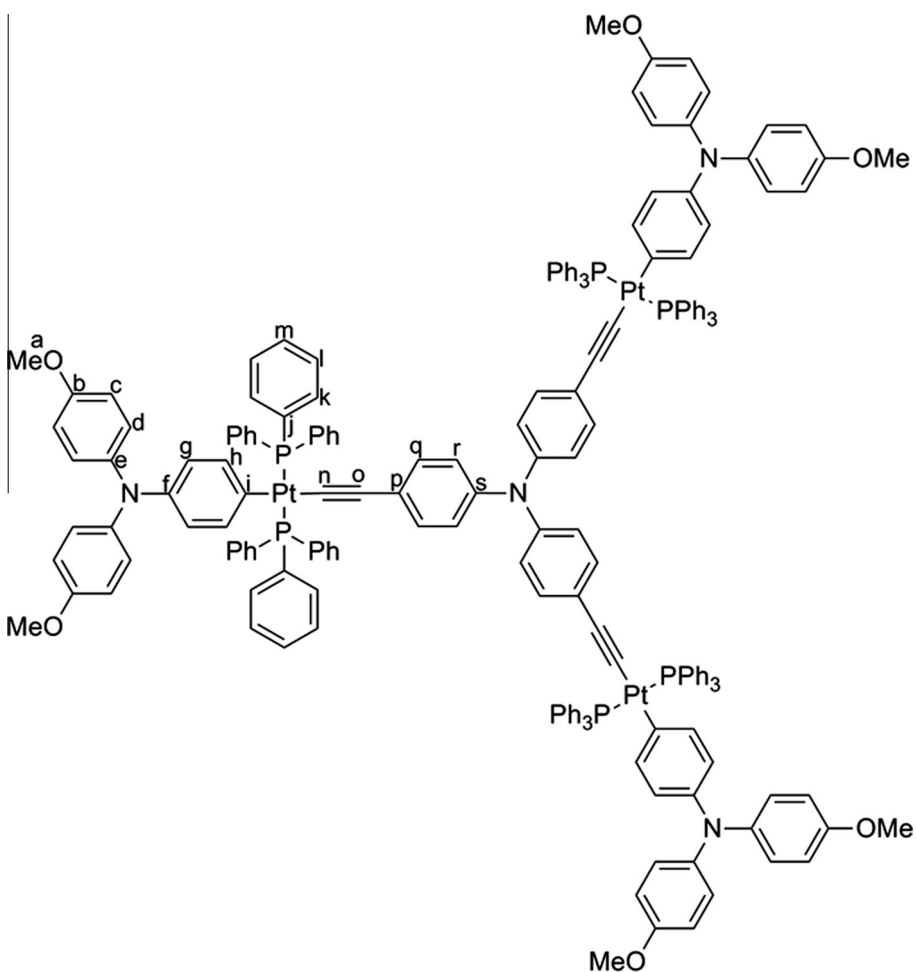
#### 4.1.6. Synthesis of *trans*-Pt(C<sub>6</sub>H<sub>4</sub>NAr<sub>2</sub>)(PPh<sub>3</sub>)<sub>2</sub><sub>2</sub>( $\mu$ -C≡C-1,4-C<sub>6</sub>H<sub>4</sub>C≡C) (5)



An oven dried Schlenk flask was charged with dry HNEt<sub>2</sub> (10 cm<sup>3</sup>) and the solvent degassed. To this solution, Pt(C<sub>6</sub>H<sub>4</sub>N(C<sub>6</sub>H<sub>4</sub>OCH<sub>3</sub>-4)<sub>2</sub>)(PPh<sub>3</sub>)<sub>2</sub> (100 mg, 0.087 mmol), CuI (3 mg) and 1,4-diethynylbenzene (5 mg, 0.043 mmol) were added and the solution stirred

at room temperature for 16 h. The precipitate was filtered, washed with ethanol (3 × 5 cm<sup>3</sup>), hexane (3 × 5 cm<sup>3</sup>) and methanol (3 × 5 cm<sup>3</sup>) and dried under airflow for 1 h. Yield 50 mg, 54%. <sup>1</sup>H NMR (CD<sub>2</sub>Cl<sub>2</sub>):  $\delta$  3.74 (s, 12H, Ha), 5.72 (s, 4H, Hq), 6.08 (d,  $J = 8$  Hz, 4H, Hh), 6.67 (d,  $J = 8$  Hz, 4H, Hg), 6.71 (m, 16H, Hc and d) 7.28 (vt,  $J = 8$  Hz, 24H, Hk), 7.37 (t,  $J = 8$  Hz, 12H, Hm), 7.59 (m, 24H, Hl). <sup>31</sup>P NMR (CD<sub>2</sub>Cl<sub>2</sub>): 20.73 ( $J_{Pt-P} = 2971$  Hz). <sup>13</sup>C NMR (CD<sub>2</sub>Cl<sub>2</sub>): 154.27 (Cb, s), 142.29 (Ce, s), 141.42 (Cf, s), 139.50 (Cg, s), 134.78 (Cl, t,  $J_{C-P} = 5$  Hz), 131.70 (Cj, t,  $J_{C-P} = 28$  Hz), 129.71 (Cq, s),

129.23 (Cm, s), 127.55 (Ck, t,  $J_{C-P} = 5$  Hz), 124.08 (Cc, s), 123.90 (Ch, s), 113.90 (Cd, s), 55.39 (Ca, s). MALDI-MS(+)  $m/z$ : 2170.6 [M]<sup>+</sup>. IR (CH<sub>2</sub>Cl<sub>2</sub>)  $\nu(C\equiv C)$  2103 cm<sup>-1</sup>. ESI-HRMS ( $m/z$ ) found 1085.8011, calculated 1085.7977.



#### 4.1.7. Synthesis of $N\{C_6H_4C\equiv Pt(C_6H_4NAr_2)(PPh_3)_2\}_3$ (**6**)

An oven dried Schlenk flask was charged with dry  $HNEt_2$  ( $10\text{ cm}^3$ ) and the solvent degassed. To this solution,  $Pt(C_6H_4N(C_6H_4OCH_3-4)_2)(PPh_3)_2$  (150 mg, 0.130 mmol),  $CuI$  (3 mg) and triethylphenylamine (13 mg, 0.043 mmol) were added and the solution stirred at room temperature for 16 h. The precipitate was filtered, washed with ethanol ( $3 \times 5\text{ cm}^3$ ), hexane ( $3 \times 5\text{ cm}^3$ ) and methanol ( $3 \times 5\text{ cm}^3$ ) and dried under airflow for 1 h. Yield 98 mg, 67%.  $^1H$  NMR ( $CD_2Cl_2$ ):  $\delta$  3.76 (s, 18H, Ha), 5.93 (d,  $J = 9\text{ Hz}$ , 6H, Hr), 6.11 (d,  $J = 8\text{ Hz}$ , 6H, Hh), 6.31 (d,  $J = 9\text{ Hz}$ , 6H, Hq), 6.69 (d,  $J = 8\text{ Hz}$ , 6H, Hg), 6.73 (m, 24H, Hc and d) 7.32 (vt,  $J = 8\text{ Hz}$ , 36H, Hk), 7.39 (t,  $J = 8\text{ Hz}$ , 18H, Hm), 7.62 (m, 36H, Hl).  $^{31}P$  NMR ( $CD_2Cl_2$ ): 20.93 ( $J_{Pt-P} = 2998\text{ Hz}$ ).  $^{13}C$  NMR ( $CD_2Cl_2$ ): 154.29 (Cb, s), 142.30 (Ce, s), 143.90 (Cs, s), 141.66 (Cf, s), 139.55 (Cg, s), 134.83 (Cl, t,  $J_{C-P} = 5\text{ Hz}$ ), 131.76 (Cj, t,  $J_{C-P} = 28\text{ Hz}$ ), 130.96 (Cr, s), 129.78 (Cm, s), 127.60 (Ck, t,  $J_{C-P} = 5\text{ Hz}$ ), 124.11 (Cc, s), 123.93 (Ch, s), 122.73 (Cq, s), 113.92 (Cd, s), 55.40 (Ca, s). MALDI-MS(+)  $m/z$ : 3385.6  $[M+H]^+$ . IR ( $CH_2Cl_2$ )  $\nu(C\equiv C)$  2105  $cm^{-1}$ . Anal. Calc. for: C, 68.10; H, 4.64; N, 1.65. Found: C, 67.87; H, 4.48; N, 1.69%.

## 5. Computational details

Full structure optimizations and analysis of all ground and excited state [74–76] properties were performed using a locally modified version of the TURBOMOLE 6.4 program code [77] enabling the use of the BLYP35 hybrid functional [78] based on

$$E_{XC} = 0.65(E_X^{LSDA} + \Delta E_X^{B88}) + 0.35E_X^{exact} + E_C^{LYP}$$

which has been shown to give accurate results for organic [78–82] and inorganic [46,83–85] MV systems. Split-valence def2-SVP basis sets were employed on all lighter atoms, together with the corresponding def2-SVP effective-core potential and a corresponding valence basis set for platinum [86–88]. Computed harmonic vibrational frequencies were scaled by an empirical factor of 0.95 [89,90]. To account for solvent effects, the conductor-like-screening (COSMO) solvent model was employed for ground state structure optimizations and analysis as well as in subsequent TDDFT calculations of excitation energies and transition dipole moments [91]. Dichloromethane ( $\epsilon = 8.93$ ) was used, as experimental data were collected in this solvent (non-equilibrium solvation was assumed in the TDDFT calculations). Spin-density and molecular-orbital isosurface plots were generated with the GaussView or Molekel programs [92]. For complex [5]<sup>+</sup> a truncated model [5-Me]<sup>+</sup>, in which the  $PPh_3$  ligands were replaced by  $PMe_3$ , was used to reduce computational cost.

## 6. Crystallographic details

The X-ray single crystal data for compounds **4a** and **4b** have been collected at 120.0 K on an Agilent XCalibur diffractometer (graphite monochromator,  $\lambda MoK\alpha$ ,  $\lambda = 0.71073\text{ \AA}$ ) equipped with a Cryostream (Oxford Cryosystems) open-flow nitrogen cryostat. The structures was solved by direct method and refined by full-matrix least squares on  $F^2$  for all data using Olex2 [93] and SHELXTL [94] software. All non-disordered non-hydrogen atoms were refined anisotropically, hydrogen atoms were placed in the calculated positions and refined in riding mode. During the preliminary stages of refinement, the extremely elongated thermal ellipsoids of carbon atoms of one of the Ph-rings in the structure **4b** indicated the disorder of the group. The different parts of the disordered group differ by their orientation around the P2–C91 bond. The disordered atoms were split in two groups and the group occupancies were allowed to refine freely while the isotropic a.d.p. of the atoms remained fixed at equal values. Then the occupancies of the disordered groups were fixed at the refined values and both

components of the disordered group were refined as regular hexagons (AFIX 66) and with isotropic a.d.p. for all carbon atoms.

### 6.1. Crystal data for **4a**

$C_{65}H_{55}NO_3P_2Pt$ ,  $M = 1155.13$ , triclinic, space group  $P\bar{1}$ ,  $a = 10.2066(3)$ ,  $b = 14.5412(4)$ ,  $c = 18.8204(6)\text{ \AA}$ ,  $\alpha = 70.667(2)^\circ$ ,  $\beta = 85.206(2)^\circ$ ,  $\gamma = 85.756(2)^\circ$ ,  $V = 2623.33(12)\text{ \AA}^3$ ,  $Z = 2$ ,  $\mu(MoK\alpha) = 2.784\text{ mm}^{-1}$ ,  $D_{calc} = 1.462\text{ g/mm}^3$ , 41162 reflections measured, 12,659 unique ( $R_{int} = 0.0472$ ) were used in all calculations. The final  $R_1$  was 0.0293 ( $>2\sigma(I)$ ) and  $wR_2$  was 0.0641 (all data).

### 6.2. Crystal data for **4b**

$C_{78}H_{66}N_2O_4P_2Pt$ ,  $M = 1352.36$ , monoclinic, space group  $P2_1/c$ ,  $a = 22.8460(15)$ ,  $b = 9.9786(5)$ ,  $c = 31.3485(17)\text{ \AA}$ ,  $\beta = 110.108(7)^\circ$ ,  $V = 6710.9(7)\text{ \AA}^3$ ,  $Z = 4$ ,  $\mu(MoK\alpha) = 2.189\text{ mm}^{-1}$ ,  $D_{calc} = 1.338\text{ g/mm}^3$ , 70643 reflections measured, 15348 unique ( $R_{int} = 0.2724$ ) were used in all calculations. The final  $R_1$  was 0.0882 (6961  $>2\sigma(I)$ ) and  $wR_2$  was 0.1729 (all data). The structure contains severely disordered solvent molecules ( $H_2O$ /methanol). Their contribution to the structural factors was taken into account by applying MASK procedure of OLEX2 program package.

## Appendix A. Supplementary data

CCDC 989928 and 989929 contains the supplementary crystallographic data for **4a** and **4b**. These data can be obtained free of charge via <http://www.ccdc.cam.ac.uk/conts/retrieving.html>, or from the Cambridge Crystallographic Data Centre, 12 Union Road, Cambridge CB2 1EZ, UK; fax: (+44) 1223-336-033; or e-mail: [deposit@ccdc.cam.ac.uk](mailto:deposit@ccdc.cam.ac.uk). Supplementary data associated with this article can be found, in the online version, at <http://dx.doi.org/10.1016/j.poly.2014.04.035>.

## References

- [1] C.R. Kistner, J.H. Hutchinson, J.R. Doyle, J.C. Storlie, *Inorg. Chem.* 2 (1963) 1255.
- [2] T.B. Peters, Q. Zheng, J. Stahl, J.C. Bohling, A.M. Arif, F. Hampel, J.A. Gladysz, *J. Organomet. Chem.* 641 (2002) 53.
- [3] Q. Zheng, J.C. Bohling, T.B. Peters, A.C. Frisch, F. Hampel, J.A. Gladysz, *Chem.-Eur. J.* 12 (2006) 6486.
- [4] D.T. Rosevear, F.G.A. Stone, *J. Chem. Soc.* (1965) 5275.
- [5] M.C. Baird, *J. Inorg. Nucl. Chem.* 29 (1967) 367.
- [6] B. Crociani, M. Nicolini, D.A. Clemente, G. Bandoli, *J. Organomet. Chem.* 49 (1973) 249.
- [7] A.J. Mukhedkar, M. Green, F.G.A. Stone, *J. Chem. Soc. A* (1970) 947.
- [8] J. Stahl, J.C. Bohling, T.B. Peters, Q.L. de, J.A. Gladysz, *Pure Appl. Chem.* 80 (2008) 459.
- [9] A.R. Norris, M.C. Baird, *Can. J. Chem.* 47 (1969) 3003.
- [10] M. Sato, E. Mogi, M. Katada, *Organometallics* 14 (1995) 4837.
- [11] M. Sato, E. Mogi, *J. Organomet. Chem.* 508 (1996) 159.
- [12] J. Manna, J.A. Whiteford, P.J. Stang, D.C. Muddiman, R.D. Smith, *J. Am. Chem. Soc.* 118 (1996) 8731.
- [13] J. Manna, C.J. Kuehl, J.A. Whiteford, P.J. Stang, *Organometallics* 16 (1997) 1897.
- [14] P. Nilsson, G. Puxty, O.F. Wendt, *Organometallics* 25 (2006) 1285.
- [15] H. Kuniyasu, F. Yamashita, T. Hirai, J.-H. Ye, S.-I. Fujiwara, N. Kambe, *Organometallics* 25 (2006) 566.
- [16] P. Nilsson, F. Plamper, O.F. Wendt, *Organometallics* 22 (2003) 5235.
- [17] T. Kondo, Y. Tsuji, Y. Watanabe, *J. Organomet. Chem.* 345 (1988) 397.
- [18] J. Manna, C.J. Kuehl, J.A. Whiteford, P.J. Stang, D.C. Muddiman, S.A. Hofstadler, R.D. Smith, *J. Am. Chem. Soc.* 119 (1997) 11611.
- [19] P.J. Stang, N.E. Persky, J. Manna, *J. Am. Chem. Soc.* 119 (1997) 4777.
- [20] D.P. Gallasch, E.R.T. Tiekink, L.M. Rendina, *Organometallics* 20 (2001) 3373.
- [21] G.R. Owen, J. Stahl, F. Hampel, J.A. Gladysz, *Chem.-Eur. J.* 14 (2008) 73.
- [22] Q.L. de, A.H. Shelton, H. Kuhn, F. Hampel, K.S. Schanze, J.A. Gladysz, *Organometallics* 27 (2008) 4979.
- [23] G.R. Owen, J. Stahl, F. Hampel, J.A. Gladysz, *Organometallics* 23 (2004) 5889.
- [24] W. Mohr, J. Stahl, F. Hampel, J.A. Gladysz, *Chem.-Eur. J.* 9 (2003) 3324.
- [25] W. Mohr, J. Stahl, F. Hampel, J.A. Gladysz, *Inorg. Chem.* 40 (2001) 3263.
- [26] T.B. Peters, J.C. Bohling, A.M. Arif, J.A. Gladysz, *Organometallics* 18 (1999) 3261.
- [27] H. Zhan, W.-Y. Wong, A. Ng, A.B. Djuricic, W.-K. Chan, *J. Organomet. Chem.* 696 (2011) 4112.

- [28] H.-M. Zhan, S. Lamare, A. Ng, T. Kenny, H. Guernon, W.-K. Chan, A.B. Djurisić, P.D. Harvey, W.-Y. Wong, *Macromolecules* 44 (2011) 5155.
- [29] L. Li, W.-C. Chow, W.-Y. Wong, C.-H. Chui, R.S.-M. Wong, *J. Organomet. Chem.* 696 (2011) 1189.
- [30] W.-Y. Wong, W.-C. Chow, K.-Y. Cheung, M.-K. Fung, A.B. Djurisić, W.-K. Chan, *J. Organomet. Chem.* 694 (2009) 2717.
- [31] W.-Y. Wong, X. Wang, H.-L. Zhang, K.-Y. Cheung, M.-K. Fung, A.B. Djurisić, W.-K. Chan, *J. Organomet. Chem.* 693 (2008) 3603.
- [32] X.-Z. Wang, W.-Y. Wong, K.-Y. Cheung, M.-K. Fung, A.B. Djurisić, W.-K. Chan, *Dalton Trans.* (2008) 5484.
- [33] L. Liu, C.-L. Ho, W.-Y. Wong, K.-Y. Cheung, M.-K. Fung, W.-T. Lam, A.B. Djurisić, W.-K. Chan, *Adv. Funct. Mater.* 18 (2008) 2824.
- [34] W.-Y. Wong, X.-Z. Wang, Z. He, K.-K. Chan, A.B. Djurisić, K.-Y. Cheung, C.-T. Yip, A.M.-C. Ng, Y.Y. Xi, C.S.K. Mak, W.-K. Chan, *J. Am. Chem. Soc.* 129 (2007) 14372.
- [35] T. Goudreault, Z. He, Y. Guo, C.-L. Ho, H. Zhan, Q. Wang, K.Y.-F. Ho, K.-L. Wong, D. Fortin, B. Yao, Z. Xie, L. Wang, W.-M. Kwok, P.D. Harvey, W.-Y. Wong, *Macromolecules* 43 (2010) 7936.
- [36] L. Liu, S.-Y. Poon, W.-Y. Wong, *J. Organomet. Chem.* 690 (2005) 5036.
- [37] S.K. Brayshaw, S. Schiffrers, A.J. Stevenson, S.J. Teat, M.R. Warren, R.D. Bennett, I.V. Sazanovich, A.R. Buckley, J.A. Weinstein, P.R. Raithby, *Chem.-Eur. J.* 17 (2011) 4385.
- [38] G.-J. Zhou, W.-Y. Wong, Z. Lin, C. Ye, *Angew. Chem., Int. Ed.* 45 (2006) 6189.
- [39] C.-L. Ho, C.-H. Chui, W.-Y. Wong, S.M. Aly, D. Fortin, P.D. Harvey, B. Yao, Z. Xie, L. Wang, *Macromol. Chem. Phys.* 210 (2009) 1786.
- [40] S.M. Aly, C.-L. Ho, W.-Y. Wong, D. Fortin, P.D. Harvey, *Macromolecules* 42 (2009) 6902.
- [41] M.S. Khan, M.K. Al-Suti, M.R.A. Al-Mandhary, B. Ahrens, J.K. Bjernemose, M.F. Mahon, L. Male, P.R. Raithby, R.H. Friend, A. Koehler, J.S. Wilson, *Dalton Trans.* (2003) 65.
- [42] M.S. Khan, M.R.A. Al-Mandhary, M.K. Al-Suti, N. Feeder, S. Nahar, A. Koehler, R.H. Friend, P.J. Wilson, P.R. Raithby, *J. Chem. Soc., Dalton Trans.* (2002) 2441.
- [43] H. Choi, C. Kim, K.-M. Park, J. Kim, Y. Kang, J. Ko, *J. Organomet. Chem.* 694 (2009) 3529.
- [44] A. Heckmann, C. Lambert, *Angew. Chem., Int. Ed.* 51 (2012) 326.
- [45] S.C. Jones, V. Coropceanu, S. Barlow, T. Kinnibrugh, T. Timofeeva, J.L. Bredas, S.R. Marder, *J. Am. Chem. Soc.* 126 (2004) 11782.
- [46] M. Parthey, K.B. Vincent, M. Renz, P.A. Schauer, D.S. Yufit, J.A.K. Howard, M. Kaupp, P.J. Low, *Inorg. Chem.* 53 (2014) 1544.
- [47] Z. He, W.Y. Wong, X.M. Yu, H.S. Kwok, Z.Y. Lin, *Inorg. Chem.* 45 (2006) 10922.
- [48] C. Lambert, G. Noll, *Angew. Chem., Int. Ed.* 37 (1998) 2107.
- [49] J.L. Song, P. Amaladass, S.H. Wen, K.K. Pasunooti, A. Li, Y.L. Yu, X. Wang, W.Q. Deng, X.W. Liu, *New J. Chem.* 35 (2011) 127.
- [50] R. Ugo, F. Cariati, G. Lamonic, *Inorg. Synth.* 28 (1990) 123.
- [51] M.S. Khan, M.R.A. Al-Mandhary, M.K. Al-Suti, F.R. Al-Battashi, S. Al-Saadi, B. Ahrens, J.K. Bjernemose, M.F. Mahon, P.R. Raithby, M. Younus, N. Chawdhury, A. Koehler, E.A. Marseglia, E. Tedesco, N. Feeder, S.J. Teat, *Dalton Trans.* (2004) 2377.
- [52] W.-Y. Wong, G.-L. Lu, K.-F. Ng, K.-H. Choi, Z. Lin, *J. Chem. Soc., Dalton Trans.* (2001) 3250.
- [53] K. Blatter, A.D. Schluter, *Synth.-Stuttgart* (1989) 356.
- [54] P.J. Low, M.A.J. Paterson, D.S. Yufit, J.A.K. Howard, J.C. Cherryman, D.R. Tackley, R. Brook, B. Brown, *J. Mater. Chem.* 15 (2005) 2304.
- [55] P.J. Low, M.A.J. Paterson, H. Puschmann, A.E. Goeta, J.A.K. Howard, C. Lambert, J.C. Cherryman, D.R. Tackley, S. Leeming, B. Brown, *Chem.-Eur. J.* 10 (2004) 83.
- [56] P.J. Low, M.A.J. Paterson, A.E. Goeta, D.S. Yufit, J.A.K. Howard, J.C. Cherryman, D.R. Tackley, B. Brown, *J. Mater. Chem.* 14 (2004) 2516.
- [57] R.E. Littleford, M.A.J. Paterson, P.J. Low, D.R. Tackley, L. Jayes, G. Dent, J.C. Cherryman, B. Brown, W.E. Smith, *Phys. Chem. Chem. Phys.* 6 (2004) 3257.
- [58] Y. Shirota, *J. Mater. Chem.* 15 (2005) 75.
- [59] S. Barlow, C. Risko, V. Coropceanu, N.M. Tucker, S.C. Jones, Z. Levi, V.N. Khurstalev, M.Y. Antipin, T.L. Kinnibrugh, T. Timofeeva, S.R. Marder, J.L. Bredas, *Chem. Commun.* (2005) 764.
- [60] S. Barlow, M.Y. Antipin, J.L. Bredas, S.J. Chung, V. Coropceanu, C. Fink, T.L. Kinnibrugh, V.N. Khurstalev, O. Kwon, S.C. Jones, Z. Levi, S.R. Marder, C. Risko, T.V. Timofeeva, N.M. Tucker, S. Zheng, E. Zojer, *Abstr. Pap. Am. Chem. S* 231 (2006).
- [61] S. Barlow, C. Risko, S.J. Chung, N.M. Tucker, V. Coropceanu, S.C. Jones, Z. Levi, J.L. Bredas, S.R. Marder, *J. Am. Chem. Soc.* 127 (2005) 16900.
- [62] N.G. Connelly, W.E. Geiger, *Chem. Rev.* 96 (1996) 877.
- [63] W.E. Geiger, F. Barriere, *Acc. Chem. Res.* 43 (2010) 1030.
- [64] F. Barriere, W.E. Geiger, *J. Am. Chem. Soc.* 128 (2006) 3980.
- [65] F. Barriere, R.J. LeSuer, W.E. Geiger, *Trends Mol. Electrochem.* (2004) 413.
- [66] F. Barriere, N. Camire, W.E. Geiger, U.T. Mueller-Westerhoff, R. Sanders, *J. Am. Chem. Soc.* 124 (2002) 7262.
- [67] P.J. Low, S. Bock, *Electrochim. Acta* 110 (2013) 681.
- [68] F. Paul, J.Y. Mevellec, C. Lapinte, *J. Chem. Soc. Dalton* (2002) 1783.
- [69] M. Parthey, J.B.G. Gluyas, P.A. Schauer, D.S. Yufit, J.A.K. Howard, M. Kaupp, P.J. Low, *Chem.-Eur. J.* 19 (2013) 9780.
- [70] P.J. Low, *Coord. Chem. Rev.* 257 (2013) 1507.
- [71] M. Kaupp, M. Renz, M. Parthey, M. Stolte, F. Würthner, C. Lambert, *Phys. Chem. Chem. Phys.* 13 (2011) 16973.
- [72] D.R. Coulson, *Inorg. Synth.* 13 (1972) 121.
- [73] C. Lambert, G. Noll, E. Schmalzlin, K. Meerholz, C. Brauchle, *Chem.-Eur. J.* 4 (1998) 2129.
- [74] R. Bauernschmitt, R. Ahlrichs, *Chem. Phys. Lett.* 256 (1996) 454.
- [75] R. Bauernschmitt, M. Haser, O. Treutler, R. Ahlrichs, *Chem. Phys. Lett.* 264 (1997) 573.
- [76] F. Furche, D. Rappoport, *Density Functional Theory for Excited States: Equilibrium Structure and Electronic Spectra*, Elsevier, Amsterdam, 2005.
- [77] TURBOMOLE V6.4 2012, a development of University of Karlsruhe and Forschungszentrum Karlsruhe GmbH, 1989–2007, TURBOMOLE GmbH, since 2007.
- [78] M. Renz, K. Theilacker, C. Lambert, M. Kaupp, *J. Am. Chem. Soc.* 131 (2009) 16292.
- [79] M. Kaupp, M. Renz, M. Parthey, M. Stolte, F. Würthner, C. Lambert, *Phys. Chem. Chem. Phys.* 13 (2011) 16973.
- [80] M. Renz, M. Kaupp, *J. Phys. Chem. A* 116 (2012) 10629.
- [81] M. Renz, M. Kess, M. Diedenhofen, A. Klamt, M. Kaupp, *J. Chem. Theory Comput.* 8 (2012) 4189.
- [82] S.F. Völker, M. Renz, M. Kaupp, C. Lambert, *Chem. Eur. J.* 17 (2011) 14147.
- [83] M. Parthey, J.B.G. Gluyas, M.A. Fox, P.J. Low, M. Kaupp, *Chem. Eur. J.*, 2014, <http://dx.doi.org/10.1002/chem.201304947>.
- [84] M. Parthey, J.B.G. Gluyas, P.A. Schauer, D.S. Yufit, J.A.K. Howard, M. Kaupp, P.J. Low, *Chem. Eur. J.* 19 (2013) 9780.
- [85] K.B. Vincent, Q. Zeng, M. Parthey, D.S. Yufit, J.A.K. Howard, F. Hartl, M. Kaupp, P.J. Low, *Organometallics* 32 (2013) 6022.
- [86] D. Andrae, U. Häussermann, M. Dolg, H. Stoll, H. Preuss, *Theor. Chim. Acta* 77 (1990) 123.
- [87] A. Schäfer, H. Horn, R. Ahlrichs, *J. Chem. Phys.* 97 (1992) 2571.
- [88] F. Weigend, R. Ahlrichs, *Phys. Chem. Chem. Phys.* 7 (2005) 3297.
- [89] A.P. Scott, L. Radom, *J. Phys. Chem.* 100 (1996) 16502.
- [90] J.C. Roder, F. Meyer, I. Hyla-Kryspin, R.F. Winter, E. Kaifer, *Chem.-Eur. J.* 9 (2003) 2636.
- [91] A. Klamt, G. Schüürmann, *J. Chem. Soc., Perkin Trans. 2* (1993) 799.
- [92] (a) R. Dennington, T. Keith, J. Millam, in: *Shawnee Mission KS, 2009.*; (b) Ugo Varetto, *MOLEKEL 5.4*, Swiss National Supercomputing Centre: Lugano (Switzerland).
- [93] O.V. Dolomanov, L.J. Bourhis, R.J. Gildea, J.A.K. Howard, H. Puschmann, *J. Appl. Crystallogr.* 42 (2009) 339.
- [94] G.M. Sheldrick, *Acta Crystallogr., Sect. A* 64 (2008) 112.